

IN-SITU MONITORING OF THICKNESS OF QUARTZ MEMBRANE DURING BATCH CHEMICAL ETCHING USING A NOVEL MICROMACHINED ACOUSTIC WAVE SENSOR

Chi-Yuan Lee¹, Tsung-Tsong Wu², Yung-Yu Chen², Shih-Yung Pao², Wen-Jong Chen¹, Ying-Chou Cheng¹, Pei-Zen Chang^{2*}, Ping-Hei Chen¹, Chih-Kung Lee², Ching-Liang Dai³, Lung-Jieh Yang⁴, Kaih-Siang Yen², Fu-Yuan Xiao², Chih-Wei Liu², Shui-Shong Lu¹

¹Department of Mechanical Engineering, National Taiwan University, Taipei, Taiwan

²Institute of Applied Mechanics, National Taiwan University, Taipei, Taiwan

³Department of Mechanical Engineering, National Chung Hsing University, Taichung, Taiwan

⁴Department of Mechanical Engineering, Tamkang University, Tamsui, Taiwan

Abstract - This work presents a novel method based on the surface acoustic wave (SAW) device for monitoring in-situ the thickness of quartz membrane during batch chemical etching. Similar to oscillators and resonators, some SAW devices require the thickness of quartz membranes to be known precisely. Precisely controlling the thickness of a quartz membrane during batch chemical etching is important, because it strongly influences post-processing and frequency control. Furthermore, the proposed micromachined acoustic wave sensor, allows the thickness of a quartz membrane from a few μm to hundreds of μm to be monitored in-situ. In particular, the proposed method is highly appropriate for monitoring in-situ a few μm thick quartz membranes, because the thickness of a quartz membrane is proportional to the phase velocity. In summary, the proposed method for measuring the thickness of quartz membrane in real time, has high accuracy, is simple to set up and can be mass produced. Also described herein are the principles of the method used, the detailed process flows, the measurement set-up and the simulation and experimental results. The theoretical and measured values differ by an error of less than $2\mu\text{m}$, so the results agreed with each other closely.

Keywords - Surface Acoustic Wave (SAW), in-situ monitoring, micromachined acoustic wave sensor

I. INTRODUCTION

Surface acoustic wave (SAW) devices, which were originally developed, and are still primarily used as high-performance signal processing element, such as filters and delay lines [1, 2]. Additionally, electronic elements based on acoustic propagation have been successfully used as filters and resonators in cellular phones, television sets and other communication systems. New development in mobile communication systems requires higher operating frequencies, smaller size and lighter equipment. Therefore, each of various oscillators and resonators must be miniature models with a high operating frequency. A higher operating frequency is obtained using a thinner substrate (quartz), because the frequency of the resonator is inversely proportional to the thickness of the membrane. Quartz has been thinned by various different techniques including chemical etching [3], plasma etching [4, 5] and mechanical polishing [6]. Chemical etching using a buffered HF solution is a method well-adapted for mass production while plasma etching provides high precision in controlling the frequency [7]. The advantages and disadvantages of wet and dry etching are well known [8]. With the mechanical restrictions on fabricating 50 MHz resonator has been the upper limit for the fundamental operating frequency at thickness of quartz about $33\ \mu\text{m}$ [9]. Even if a thinner

substrate could be lapped and polished, implementing mass production and ensuring high reliability would be difficult.

Chemical etching was the key technology for fabricating each of the various SAW devices (oscillators and resonators) on quartz substrate. A high frequency fundamental (HFF) quartz resonator with a frequency range from 80MHz to nearly 1GHz in the fundamental mode, is fabricated by an industrial photolithographic batch manufacturing process with chemical etching [9]. So, the in-situ precise monitoring of the thickness of a quartz membrane during batch chemical etching is important, because the thickness strongly influences post-processing and frequency control. Most of today's available techniques are limited by the lack of adequate in-situ measurement methods. Overcoming the shortcoming of all of these manufacturing methods, this work developed a novel method for measuring the thickness of quartz membrane in situ, with high accuracy, a simple setup and the capacity for mass production.

II. DESIGN

A. Surface waves that propagate in a piezoelectric plate loaded with viscous liquid

In this paper, the eight-dimensional matrix formalism was applied to study surface wave propagation in piezoelectric plates loaded with viscous liquid [10]. The dispersion equation of surface waves in such a structure is formulated from the continuity conditions at the solid-liquid interface. With this formulation, the size of the matrix encountered in the computation is independent of the number of layers.

Consider a piezoelectric plate loaded with viscous liquid in the half-space, where the interface is at $z = H$ as shown in Figure 1. According to the eight-dimensional matrix formalism, at the interface, the relationship between the generalized traction vector \mathbf{T} and the generalized velocity vector \mathbf{V} is expressed as

$$\mathbf{T}(H^-) = \mathbf{G} \mathbf{V}(H^-) \quad (1)$$

where \mathbf{G} is the 4×4 impedance tensor, and H is the plate thickness. In the viscous liquid half-space, because only up-going waves exist, the global impedance is equivalent to the up-going wave impedance \mathbf{Z}_1 . Therefore, the corresponding relation at the boundary of the viscous liquid is given by

$$\mathbf{T}_1(H^+) = \mathbf{Z}_1 \mathbf{V}_1(H^+) \quad (2)$$

At the liquid-solid interface, the stress, the particle velocity, the electric potential and the electric displacement must satisfy the continuity condition:

$$\mathbf{T}(H^-) = \mathbf{T}_1(H^+) \quad , \quad \mathbf{V}(H^-) = \mathbf{V}_1(H^+) = \mathbf{V}(H) \quad (3)$$

From equations (1), (2), and (3), we obtain that

$$(\mathbf{G} - \mathbf{Z}_1) \mathbf{V}(H) = \mathbf{0} \quad (4)$$

The non-trivial solution of the generalized velocity vector $\mathbf{V}(H)$ exists only if

$$\det(\mathbf{G} - \mathbf{Z}_1) = 0 \quad (5)$$

Equation (5) is also called the dispersion equation for the propagation of surface waves in a piezoelectric plate loaded with viscous liquid half-space. The generalized velocity vector at the liquid-solid interface can be obtained by substituting in the wave number k_x in the x -direction and the circular frequency ω , both of which satisfy equation (5). The generalized traction vector at the interface can be determined by substituting the generalized velocity vector into equation (4). Once the two generalized vector are known, the stress, the particle velocity, the electric potential and the electric displacement at any position in the liquid or solid part can be evaluated.

Here, the formulation based on the surface impedance tensor method was utilized to calculate the

dispersion curve of the air or the viscous liquid loaded AT-cut quartz substrate. Figures 2(a) and 2(b) present the simulation results, which are phase velocity with respect to the product of the wave number and the quartz thickness, respectively. According to the simulation results, the phase velocity approaches the velocity of the Rayleigh wave of quartz when the product of the wave number and the thickness of the quartz become larger in air. Similarly, the phase velocity approaches the traveling velocity of the liquid when the product of the wave number and the thickness of the quartz become larger in liquid. When the quartz is thinner the wavelength of the surface acoustic wave, the surface acoustic wave and the bulk wave combine into a plate wave, and the phase velocity changes with the thickness of the quartz substrate.

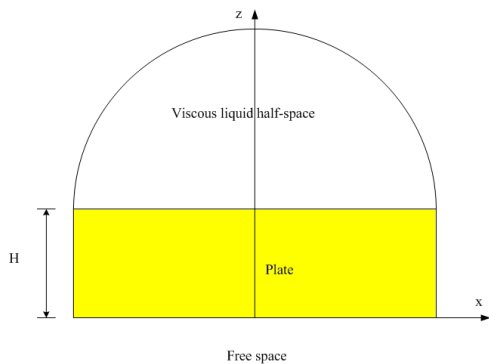
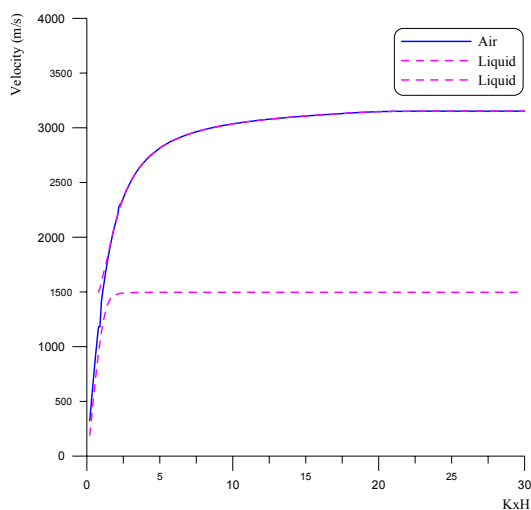
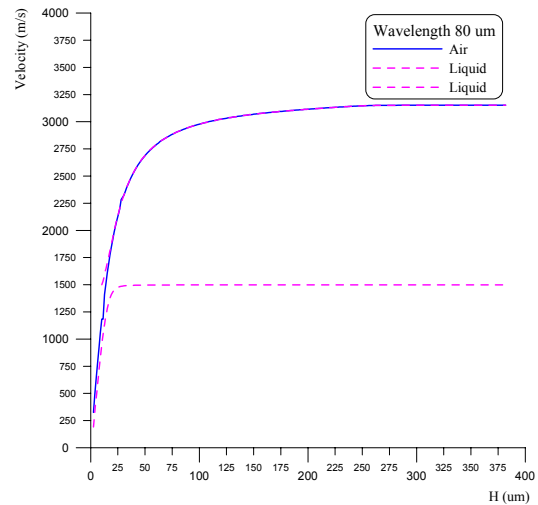


Fig. 1. Configuration of a piezoelectric plate loaded with viscous liquid in the half-space.



(a) Dispersion curve of the product of wave number and quartz thickness versus phase velocity



(b) Dispersion curve of thickness of quartz versus phase velocity

Fig. 2. Dispersion curve of the air or the viscous liquid loaded AT-cut quartz substrate.

B. Design of micromachined acoustic wave sensor

A surface acoustic wave (SAW), also called a Rayleigh wave, is essentially a coupling between longitudinal and shear waves. The energy carried by the SAW is confined near the surface. An associated electrostatic wave exists for a SAW on a piezoelectric substrate, which allows electroacoustic coupling via a transducer [11]. Quartz has been the material of choice since its high Q (quality factor) and high stiffness makes it the primary frequency and frequency-stability determining element in a crystal oscillator. A micromachined acoustic wave sensor was made on AT-cut quartz substrate using two-ports of split-electrode interdigital transducers (IDT). The piezoelectric effect is such that, when the AC voltage was applied to the split-electrode of the input IDT, and

signal voltage variations were subsequently converted into a mechanical acoustic wave, the other IDT was used as an output receiver to convert mechanical SAW vibrations back into output voltage [12]. The output voltage or the wave velocity change with the thickness of the quartz substrate.

Figure 3 sketches of configuration of the IDT, where λ is the periodicity of IDT (wavelength of the surface acoustic wave), L is the length of the IDT fingers, W is the length of overlap of the IDT fingers (acoustic aperture), and d is the length of the path of acoustic propagation. In the design of IDT, a number of parameters have to be specified. The spacing and the electrode width will determine the frequency response of the transducer. In the proposed design, a split-electrode IDT was selected, because the problem that results from finger reflections can be greatly diminished using a $\lambda/8$ finger width instead of a $\lambda/4$ finger width, such that the SAW reflections from each split-electrode pair cancel out at the center frequency, rather than adding as in the case of the single-electrode IDT [12]. Table 1 list the parameters of the IDT design used in our experiment.

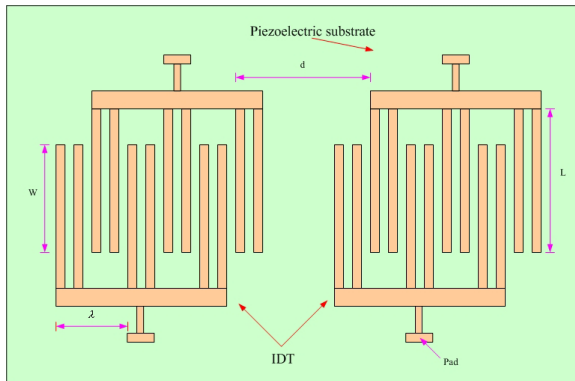


Fig. 3. Sketches of configuration of the IDT.

Tab. 1. IDT design parameters

Interdigital transducer (IDT)	Value of parameter
Numbers of pairs (N)	80
Periodicity of IDT(λ)	80 μm
Length of the IDT fingers (L)	3600 μm
Length of overlap of the IDT fingers (W)	2800 μm
Length of the path of acoustic propagation (d)	1200 μm
Area of pad	80 $\mu\text{m} \times 80 \mu\text{m}$

III. FABRICATION

This novel micromachined acoustic wave device was fabricated by the process illustrated in Fig. 4. The process was begun with an AT-cut 392 μm thick of 76 mm diameter quartz. First, on the rear side of the quartz substrate, the Shipley S1813 photoresist was coated using a spinner that rotated at a rate of 1000 rpm for 5 seconds, and then 4000 rpm for 40 seconds. The coated substrate was then softbaked at 90 $^{\circ}$ for 100 seconds. Besides of etching-hole area pattern was exposed onto the photoresist coated substrate surface by using ultraviolet light. To increase the adhesion of an Au film, a Cr film of about 100 \AA thick was evaporated before an Au film with a thickness of 900 \AA was evaporated: both processes involved a thermal evaporator, as shown in Fig. 5(a). The unwanted Cr and Au films were lifted off by soaking the substrate in acetone to form a rear side etching-hole, as shown in Fig. 5(b). Care was taken to ensure the success of the lift-off process. Several causes of failure of lift-off may apply, such as a lack of an undercut photoresist pattern, non-vertical evaporation of Au, poor Au film adhesion and substrate surface contamination [13]. Au film was used as an etching mask during wet etching in NH_4HF_2 solution. IDTs were patterned using semiconductor photolithographic techniques, which involved the deposition of a thickness of 900 \AA of Al by electron beam evaporation, as shown in Fig. 5(c). Finally,

a quartz membrane was formed by soaking the rear side of the substrate in NH_4HF_2 solution, as shown in Fig. 5(d).

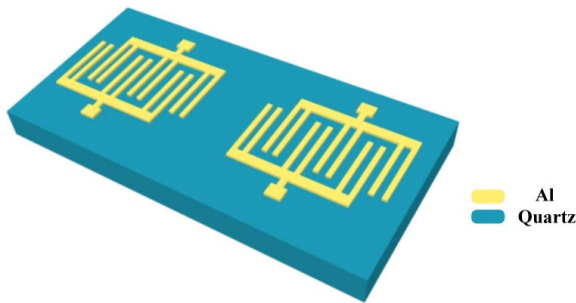


Fig. 4. Schematic diagram of a micromachined acoustic wave device.

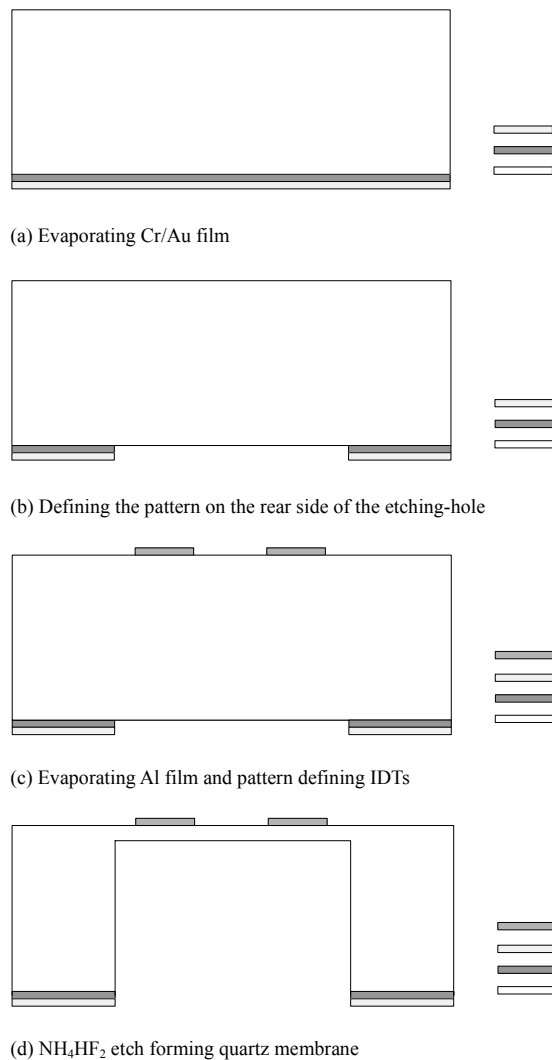


Fig. 5. Process flow of a micromachined acoustic wave device.

IV. RESULTS

The experimental setup for measuring the frequency response and the insertion loss for a micromachined acoustic wave device, as illustrated in Fig. 6, includes a HP8714ES network analyzer and an etching holder. An HP8714ES network analyzer monitor was used to monitor in real time the thickness of the quartz membrane as the target central frequency was shifted. When the central frequency shifts, the thickness of the quartz membrane can be determined based on the amount of shift of the central frequency. The etching process automatically monitors the thickness of the quartz membrane as the frequency changes. First, the Alpha-step 500 surface profiler was used to measure the initial total thickness of 392 μm thick AT-cut quartz, as shown in Fig. 7(a). Then, μ scan AF2000 was used to measure the initial thickness of the unetched rear side of the quartz, which was 883.524 μm thick, as shown in Fig. 7(b). The central frequency of experimental unetched was 39.406MHz, as shown in Fig. 7(c). Similarly, the first etched rear side of quartz was measured at 951.63 μm thick, as shown in Fig. 7(d). An experimental result of first etched central frequency was 39.406MHz, as shown in Fig. 7(e). According to Figs. 7(a), (b) and (d), the thickness of the quartz membrane can be determined now. Repeat steps, the second etched rear side of quartz was measured at

1010.445 μm thick, as shown in Fig. 7(f). An experimental result of second etched central frequency was 39.375MHz, as shown in Fig. 7(g). Figure 8 compares the simulation and experimental results of quartz thickness with respect to frequency. Figure 8 reveals that the error between simulation and experimental results is within the 2 μm , implying close correspondence.

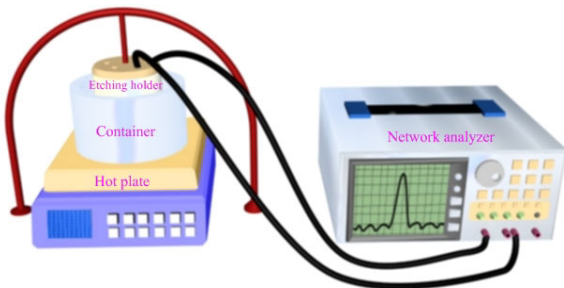
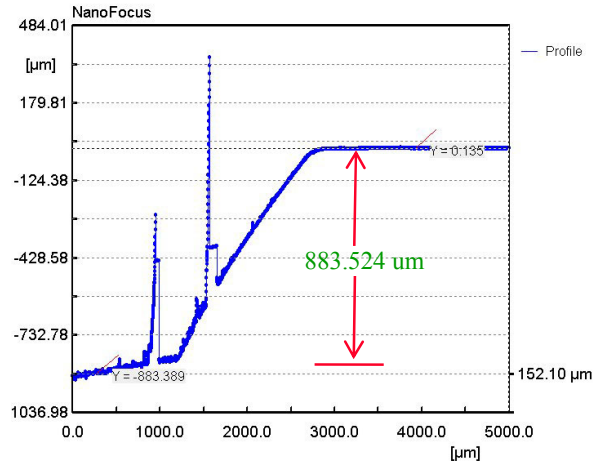


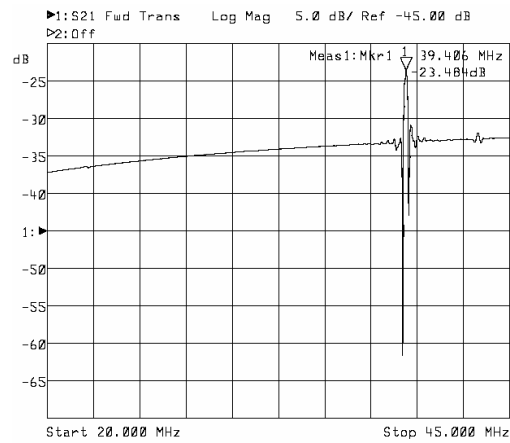
Fig. 6. Experimental setup of a micromachined acoustic wave device.



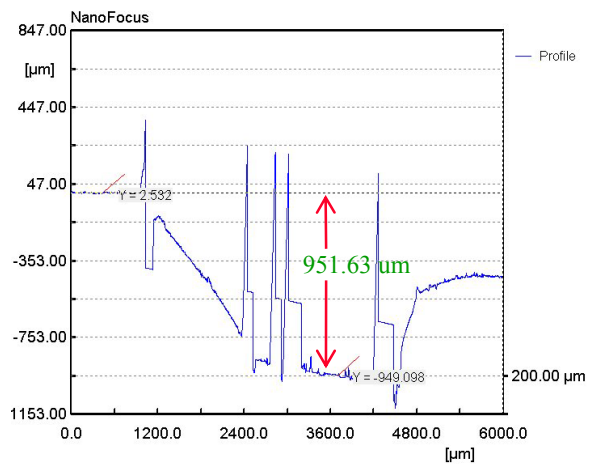
(a) Photograph of initial total thickness of unetched quartz, obtained by surface profiler



(b) Photograph of initial thickness of unetched rear side of quartz, obtained by μ scan AF2000

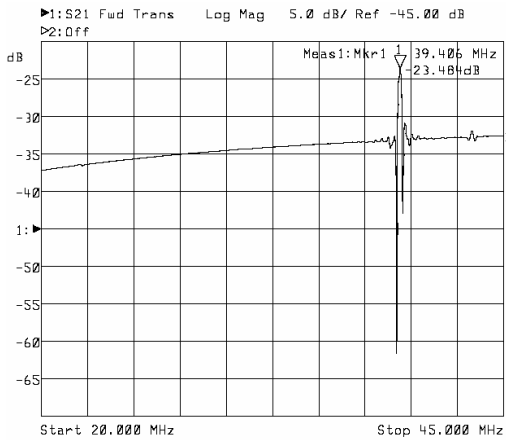


(c) Experimental results of unetched central frequency versus insertion loss

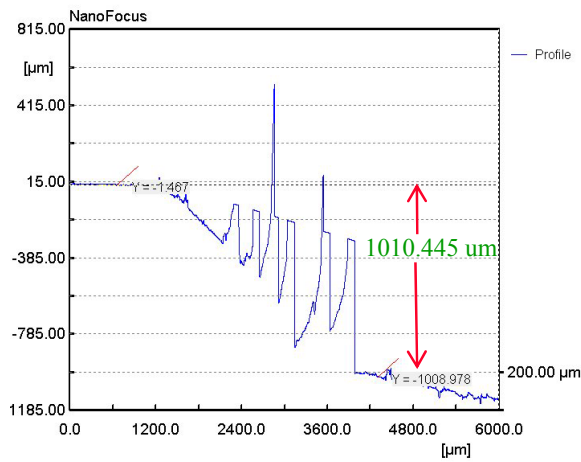


(d) Photograph of thickness of first etched rear side of quartz, obtained

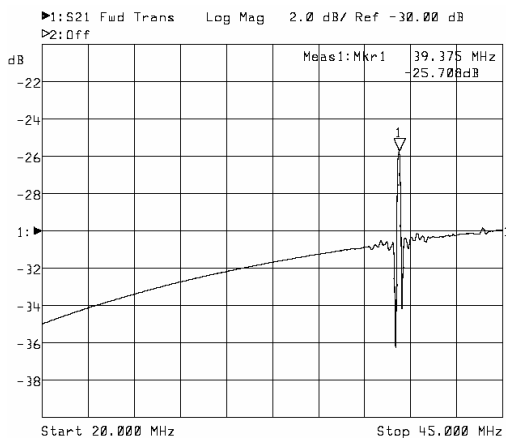
by μ scan AF2000



(e) Experimental results of first etched central frequency versus insertion loss



(f) Photograph of thickness of second etched rear side of quartz, obtained by μ scan AF2000



(g) Experimental results of second etched central frequency versus insertion loss

Fig. 7. Experimental results with unetched and etched for the

central frequency versus insertion loss, and photographs of the thickness of quartz membrane obtained by μ scan AF2000.

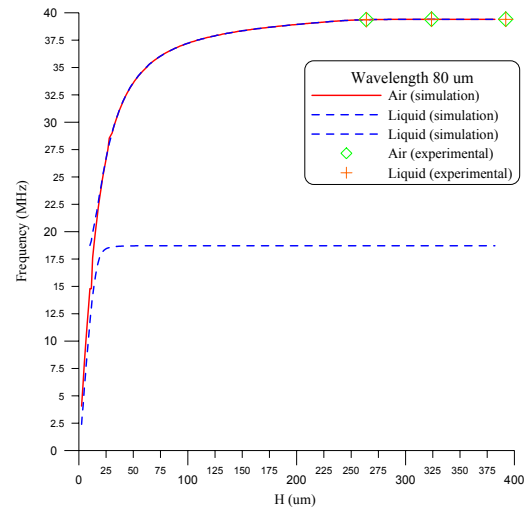


Fig. 8. Comparison of simulation and experimental results of thickness of quartz with respect to frequency.

V. CONCLUSION

In this work presents a novel micromachined acoustic wave sensor for monitoring the thickness of a quartz membrane in real time during wet etching. Also described herein are the principles of the method used, the detailed process flows, the measurement set-up, and the simulation and experimental results. The error between the theoretical and measured values is within $2\mu\text{m}$, implying close correspondence.

ACKNOWLEDGMENT

This work was accomplished with much needed support and the authors would like to thank Dr. Jen-Yi Chen, Dr. Chien-Liu Chang, Dr. Chin-Wei Wu, Dr. Yuh Chung Hu, Dr. Chyan-Chyi Wu, Hun-Lin Chen, Jing-Hung Chiou, Tsung-Wei Huang, Shih-Chen Chang, Chun-Yuan Chi, Chia-Hua Chu of the Institute of Applied Mechanics, National Taiwan University, for their valuable advice and assistance in experiment. In addition, we would, finally, like to thank the NSC Northern Region MEMS Research Center for kindly making their complete research facilities available.

REFERENCES

- [1] D. P. Morgan, "Surface wave devices for signal processing," Elsevier, Amsterdam, 1985.
- [2] C. K. Campbell, "Surface wave devices and their signal processing applications," Academic Press, Boston, 1989.
- [3] O. Ishii, T. Morita, T. Saito, and Y. Nakazawa, "High frequency fundamental resonators and filters fabricated by batch process using chemical etching," *IEEE International frequency control symposium*, 1995, pp. 818-826.
- [4] K. M. Lakin, G. R. Kline, and K. T. McCarron, "Self limiting etching of piezoelectric crystals," *IEEE International frequency control symposium*, 1995, pp. 827-831.
- [5] Y. Nagaura and S. Yokomizo, "Manufacturing method of high frequency quartz oscillators over 1GHz," *IEEE International frequency control symposium*, 1999, pp. 425-428.
- [6] Y. Nagaura, K. Kinoshita, and S. Yokomizo, "High-frequency, plano-convex quartz oscillators made by a dual-face lapping machine," *IEEE/ELA International frequency control symposium and exhibition*, 2000, pp. 255-259.
- [7] C. Wuthrich, S. D. Piazza, U. Ruedi, and B. Studer, "Batch fabrication of AT-cut crystal resonators up to 200 MHz," *IEEE International frequency control symposium*, 1999, pp. 807-810.
- [8] K. R. Williams and R. S. Muller, "Etch rates for micromachining processing," *Journal of Microelectromechanical systems*, vol. 5, 1996, pp. 256-269.
- [9] O. Ishii, H. Iwata, M. Sugano, and T. Ohshima, "UHF AT-cut crystal resonators operating in the fundamental mode," *IEEE International frequency control symposium*, 1998, pp. 975-980.
- [10] T. T. Wu and M. P. Chang, "Surface waves in layered piezoelectric medium loaded with viscous liquid," *Jpn. J. Appl. Phys.* (accepted).
- [11] K. Uchino, "Ferroelectric devices," Marcel Dekker, New York, 2000.
- [12] C. K. Campbell, "Surface Acoustic Wave Devices for Mobile and Wireless Communication," Academic Press, New York, 1998.
- [13] S. M. Sze, "VLSI technology," McGraw-Hill, New York, 1988.

* E-mail: changpz@mems.iam.ntu.edu.tw